An Upcycling Strategy for Polyethylene Terephthalate Fibers: All-Polymer Composites with Enhanced Mechanical Properties

Journal of
Composites Science

MDPI

Article

An Upcycling Strategy for Polyethylene Terephthalate Fibers: All-Polymer Composites with Enhanced Mechanical Properties

Chiara Gnoffo [1,2], Rossella Arrigo [1,2] and Alberto Frache [1,2,*]

[1] Dipartimento di Scienza Applicata e Tecnologia, Politecnico di Torino, Viale Teresa Michel 5, 15121 Alessandria, Italy; chiara.gnoffo@polito.it (C.G.); rossella.arrigo@polito.it (R.A.)
[2] Local INSTM Unit, Viale Teresa Michel 5, 15121 Alessandria, Italy
* Correspondence: alberto.frache@polito.it

Abstract: In this work, an effective route for achieving high-performance all-polymer materials through the proper manipulation of the material microstructure and starting from a waste material is proposed. In particular, recycled polyethylene terephthalate (rPET) fibers from discarded safety belts were used as reinforcing phase in melt-compounded high-density polyethylene (HDPE)-based systems. The formulated composites were subjected to hot- and cold-stretching for obtaining filaments at different draw ratios. The performed characterizations pointed out that the material morphology can be profitably modified through the application of the elongational flow, which was proven able to promote significant microstructural evolutions of the rPET dispersed domains, eventually leading to the obtainment of micro-fibrillated all-polymer composites. Furthermore, tensile tests demonstrated that hot-stretched and, especially, cold-stretched materials show significantly enhanced tensile modulus and strength as compared to the unfilled HDPE filaments, likely due to the formation of a highly oriented and anisotropic microstructure.

Keywords: all-polymer composites; polyethylene terephthalate; high-density polyethylene; mechanical recycling; waste valorization; elongational flow; micro-fibrillation

Citation: Gnoffo, C.; Arrigo, R.; Frache, A. An Upcycling Strategy for Polyethylene Terephthalate Fibers: All-Polymer Composites with Enhanced Mechanical Properties. *J. Compos. Sci.* **2024**, *8*, 527. https://doi.org/10.3390/jcs8120527

Academic Editors: Francesco Aymerich and Pietro Russo

Received: 8 November 2024
Revised: 29 November 2024
Accepted: 12 December 2024
Published: 14 December 2024

1. Introduction

The worldwide production of plastic has shown a steadily increasing trend in recent decades; according to the latest available data, the world's plastic production reached 400.3 Mt in 2022, of which almost 25% was sent to landfill [1]. Although in recent years a significant increase in the use of post-consumer mechanically recycled plastics was observed, there are many technological obstacles strongly affecting the achievement of a full plastic circularity. The main issues still limiting the effective utilization of recycled plastics are mainly related to the gradual loss of properties, hence of added value, when polymers are subjected to mechanical recycling processes [2]. In fact, the thermo-degradation reactions experienced by polymers during re-processing, coupled with the different forms of degradation (such as thermo- or photo-oxidation and hydrolyzation) that plastic materials undergo during their lifetime, cause a progressive modification of the macromolecular architecture of the polymer chains, as well as of their chemical structure, thereby affecting the processability and final properties of the recyclates [3,4]. For all these reasons, mechanical recycling is usually considered a downcycling process, given that poor-quality recycled polymers can be further exploited for applications with fewer engineering requirements as compared to those of the original ones [5].

Polyethylene terephthalate (PET) represents one of the most exploited plastics. In 2022, 5 million tonnes of PET for packaging applications (encompassing bottles, trays and flexibles) and about 3.2 million tonnes of PET-based synthetic textiles were placed on the European market [6]. Although in recent decades several effective mechanical recycling strategies have been developed for PET, high recycling rates are currently achieved solely

for the recovery of PET bottles (50–55%) and trays (about 20%). Conversely, the recycling rate for PET filaments and textiles is below 10%, and less than 1% are recycled following closed-loop strategies [7]. In fact, when post-consumer PET textiles are mechanically recycled, the recovered material is usually employed for the production of low-added-value products, such as insulation materials and wiping cloths [7]. Interestingly, it has been demonstrated that recycled PET (rPET) recovered from different sources can be exploited as reinforcing phase in polymer–polymer fibrillated composites [8–10]. These systems are usually formulated by exploiting the deformation of polymer particles characterized by a high crystallinity dispersed in a viscous molten matrix [11]. In this way, micro- or nano-fibrils are generated in situ during the processing step, allowing high-performance reinforced systems to be obtained while avoiding the utilization of potentially hazardous nanofillers, and maintaining, at the same time, the recyclability of the polymer matrix [12]. Alternatively, fibrillated all-polymer composites can also be achieved by subjecting to the elongational flow an immiscible polymer blend characterized by a typical droplet–matrix morphology [13]. In this case, the applied stretching induces the deformation and elongation of the droplet of the dispersed phase, bringing about the formation of anisotropic fibrils embedded within an isotropic matrix. Obviously, the mechanism of in situ fiber formation requires the elongation of the particles of the dispersed phase rather than their breakup; therefore, it is effective if the polymer constituting the dispersed phase presents proper rheological characteristics [14]. In this context, it has been shown that rPET/polypropylene fibrillated composites can be successfully obtained by melt spinning starting from a melt-compounded blend, due to the morphological evolution of rPET dispersed particles upon drawing [15]. Similarly, Liu et al. [16] demonstrated the achievement of high-aspect-ratio rPET fibrils in a ternary blend based on polypropylene and polyethylene via a hot-stretching process. Interestingly, it was found that the presence of the rPET fibrils prevents the relaxation of the macromolecules of the polyolefin matrices stretched by the applied elongational flow, promoting the achievement of a highly oriented microstructure which imparts enhanced tensile properties to the fibrillated all-polymer composite.

The main scope of this study is to explore the possibility of developing all-polymer composites starting from a high-density polyethylene (HDPE) matrix and rPET fibers recovered from discarded safety belts. The underlying idea is taking advantage of a potential reinforcing phase that is already in the form of anisotropic fibers for obtaining all-polymer fibrillated systems. Firstly, HDPE/rPET all-polymer composites were melt-processed at three different temperatures, aiming at assessing the possible effect of the processing conditions on their morphology and tensile properties. Finally, the material obtained at the highest processing temperature was further subjected to hot- and cold-stretching, and the obtained results demonstrated that the elongational flow can be profitably exploited to promote the microstructural evolution of the dispersed phase, eventually leading to the obtainment of micro-fibrillated composites. In all, an effective and easily viable upcycling strategy is proposed, providing novel insights for an effective valorization of a waste polymer usually exploited for low-added-value applications, such as PET fibers recovered from textiles.

2. Materials and Methods

2.1. Materials

The materials used in this work were as follows:

- High-density polyethylene (HDPE) Lupolen 4261AG (Melt Flow Rate (190 °C/21.6 kg) 6 g/10 min, density 0.945 g/cm^3), supplied by LyondellBasell and used as matrix.
- rPET fibers, recovered from discarded safety belts of cars collected from local junkyards. According to the calorimetric characterization, the fibers have a melting temperature of 251.6 °C (T_{ONSET} = 227.4 °C; T_{ENDSET} = 261.3 °C).

2.2. All-Polymer Composite Preparation

As a first step, a masterbatch containing 20 wt% of rPET fibers was obtained by using a Brabender internal mixer operating at 200 °C and at a rotation speed of 30 rpm for 360 s. Subsequently, a twin-screw extruder Process 11 (ThermoFisher Waltham, MA, USA) was employed to obtain all-polymer composite systems containing 5 wt% of rPET fibers. The materials were processed using three flat temperature profiles at 30 rpm and constant feed rate. In particular, the selected processing temperatures were as follows: (i) 220 °C, which is below the melting temperature (T_M) of rPET fibers; (ii) 240 °C, which is below the T_M while above the onset temperature of the melting peak of rPET fibers; and (iii) 260 °C, above the T_M of rPET fibers.

Hereinafter, the obtained all-polymer systems will be named HDPE/rPET_X °C, with X denoting the processing temperature. The pristine HDPE matrix was processed at 220 °C while keeping all the other parameters unchanged.

The hot-stretching step was performed by subjecting HDPE/rPET_260 °C extrudates to non-isothermal elongational flow using an IdeaInstr (Italy) RheoSpin apparatus (described in detail in [17]) in order to collect filaments at different draw ratios (DR_H = $diameter^2_{extrudate}/diameter^2_{fiber}$, with $diameter_{extrudate}$ being 1.5 mm). On the other hand, cold-stretching was carried out exploiting an Instron 5966 dynamometer by stretching filaments (with a DR_H = 1 and a length of 2 cm) up to obtain a cold draw ratio DR_C ($DR_C = l_{final}/l_{initial}$) equal to 3, 5 and 6.

2.3. Characterization Techniques

For the rheological characterization, an ARES (TA Instruments) parallel-plate rotational rheometer (plate diameter = 25 mm) was employed. Preliminary strain sweep tests were conducted at 220 °C at a frequency of 10 rad/s and strain values between 0.1 and 300%; afterwards, frequency sweep tests were carried out with frequency ranging from 100 rad/s to 0.01 rad/s, by imposing a strain amplitude in the linear viscoelastic region for all samples. The experimental complex viscosity data were fitted with the Carreau–Yasuda rheological model (Equation (1)):

$$\eta^*(\omega) = \eta_0{}^* \left[1 + (\lambda\omega)^a\right]^{\frac{n-1}{a}} \quad (1)$$

where $\eta^*(\omega)$ is the complex viscosity as a function of the frequency, η_0 is the zero-shear viscosity, λ is the relaxation time, n is the power-law index and a is a fitting parameter.

Specimens for the rheological tests were produced through a compression molding step, using a hot-plate press P200T Collins at 200 °C and 100 bar with 3 min of preheating and 2 min of pressing.

The tensile characterization has been performed on three different specimens: (i) isotropic samples (obtained through compression molding from the extrudates) on dog-bone specimens having overall length of 75 mm and width of 4 mm, with a gauge length of 20 mm; (ii) hot-stretched filaments having different DR_H; and (iii) cold-stretched filaments at different DR_C.

A 5966 Instron dynamometer with a 2kN load cell was used for the mechanical tests, which were carried out at room temperature using a 1 mm/min rate until 0.05% deformation was reached; then, the crossover speed was increased up to 10 mm/min until the specimen broke. At least five specimens were tested for each kind of sample and the results averaged.

Morphological observations were performed through a Evo 15 Zeiss Scanning Electron Microscope (SEM) on surfaces that had previously been brittle-fractured by treating them with liquid nitrogen and coated with a thin layer of gold.

3. Results and Discussion

3.1. Characterization of the Melt-Compounded (Isotropic) HDPE/rPET All-Polymer Materials

3.1.1. Morphological Observations

Firstly, the morphology of the materials obtained through the melt-compounding step at three different processing temperatures was assessed through SEM observations and the obtained micrographs are shown in Figure 1. Significant variations can be noticed in the morphology of the all-polymer composites processed at temperatures lower than the melting temperature of rPET and the one related to HDPE/rPET_260 °C. In particular, the systems extruded at 220 and 240 °C (see Figures 1a, 1b and 1c, respectively) exhibited a quite similar morphology, and the fiber-shape of the original rPET fibers was maintained since they were still preserved in a solid state during the processing. The average diameter of rPET fibers amounted to about 70 and 52 μm for the materials processed at 220 and 240 °C, respectively, and this slight reduction noticed for the system obtained at higher temperature can be likely attributed to the processing temperature approaching the rPET melting peak. On the other hand, when the highest processing temperature (i.e., 260 °C) was exploited, the sample presented a significantly different microstructure. In fact, as observable in Figure 1d, HDPE/rPET_260 displays the typical droplet-like morphology of an immiscible blend, distinguished by a homogeneous and continuous matrix phase in which the roughly spherical domains of the dispersed phase are embedded [18,19]. In this case, due to the processing temperature being higher than the melting temperature of the rPET, the formation of spherical particles (characterized by an average diameter ranging from 0.5 to 2.5 μm) arose.

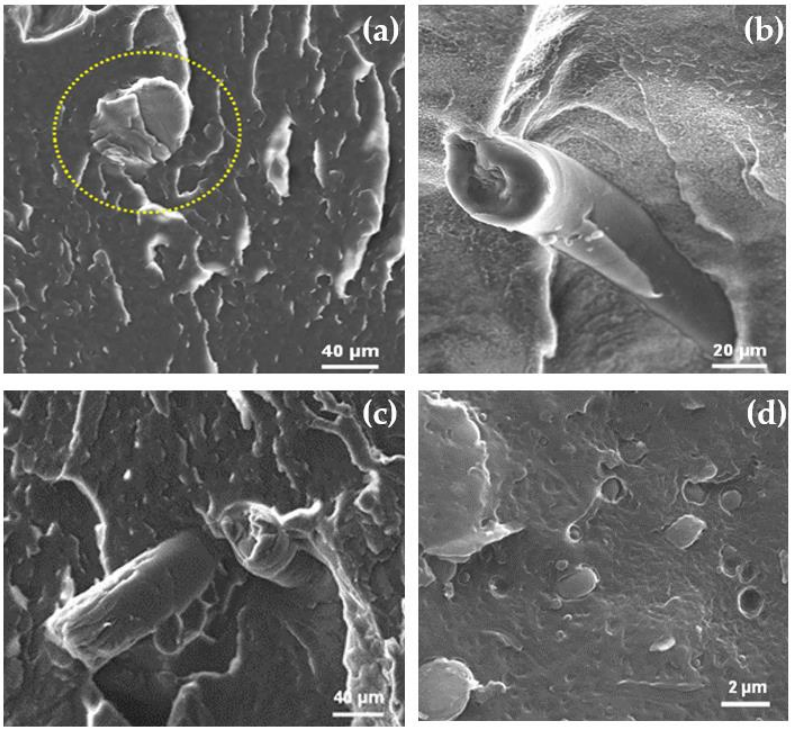

Figure 1. SEM micrographs for HDPE/rPET extrudates processed at 220 (**a**,**b**), 240 (**c**) and 260 (**d**) °C.

3.1.2. Rheological Behavior

Given that the SEM observations demonstrated the achievement of different morphologies depending on the processing temperatures, the samples collected after the melt-compounding step were characterized from a rheological point of view, in order to gain further insights into the processing/microstructure relationships.

Figure 2 reports the trends of the complex viscosity (η*) and of the storage modulus (G′) curves as a function of the frequency (ω) for unfilled HDPE and HDPE/rPET systems

extruded at the three different temperatures. First of all, it is important to highlight that neat HDPE, as far as the complex viscosity is concerned, exhibited a remarkable non-Newtonian behavior in the whole investigated frequency range. The observed trend can be related to the high molecular weight of the exploited polymer, as suggested by its relatively low MFI value (i.e., 6 g/10 min). In fact, the presence of long chains implies the formation of a dense entanglement network that prevents the full relaxation of the macromolecules in the tested time interval [20]. The introduction of rPET fibers caused the occurrence of different variations in the complex viscosity curve of HDPE, depending on the compounding temperature (Figure 2a–c). From a general point of view, the effect of the rPET phase on the rheological behavior of the matrix was appreciable in the low-frequency region, while at high frequencies, the rheological response of the all-polymer composites was governed by that of the matrix, irrespective of the processing temperature. Looking at the low-frequency region, the systems obtained at different temperatures presented a very similar complex viscosity trend. More specifically, as compared to the unfilled HDPE, the three materials exhibited a more pronounced non-Newtonian behavior, involving higher values of zero-shear viscosity and a sharper decrease in the complex viscosity as the frequency increased. Both these features can be quantitatively evaluated through the fitting of the viscosity curves performed through the Carreau–Yasuda model. In fact, as observable from Table 1, in which the fitting parameters are listed, these samples show higher values of η_0 and of the shear-thinning index with respect to the unfilled HDPE. Similar conclusions can be drawn from the analysis of the storage modulus curves as a function of the frequency reported in Figure 2d–f. Also in this case, in fact, regardless the processing temperature, the presence of the rPET phase induced a more notable non-terminal behavior in the HDPE/rPET materials, as demonstrated by the lower slope of the G' curves in the terminal region as compared to the unfilled HDPE; this last indicates a more pronounced solid-like behavior for the all-polymer composites [21]. The rheological response of the HDPE/rPET systems can be explained considering the different microstructures of the samples obtained at the three processing temperatures. In particular, in the samples processed at 220 °C (i.e., below the melting point of rPET), the rPET fibers remained in the solid state during the processing and, as the SEM analysis demonstrated (see the micrograph shown in Figure 1a,b), they preserved their original shape in the final extrudates. Therefore, in this case, the dispersed phase is believed to act as a "classical" solid filler that slows down the relaxation dynamics of the HDPE chains, inducing more prominent non-Newtonian behavior and solid-like response with respect to the unfilled matrix (as reported in Figure 2a,d). Differently, the material processed at 260 °C (i.e., above the melting temperature of the rPET) was actually an immiscible polymer blend, showing a matrix–droplet morphology (see SEM micrograph shown in Figure 1d) typical of such systems. In this case, therefore, the different rheological behavior of this material as compared to the unfilled matrix is attributable to the biphasic microstructure of the material, in which the existence of an interfacial region between the two phases and the shape relaxation of the dispersed rPET droplets induce an overelasticity, resulting in the increase in the complex viscosity and of the storage modulus in the low-frequency region, as shown in Figure 2c,f, respectively [22]. Finally, for the sample obtained at 240 °C, the morphological analysis (see Figure 1c) documented the obtainment of a microstructure very similar to that of HDPE/rPET_260 °C. However, in this case, less marked non-Newtonian characteristics and solid-like behavior were recorded, likely due to the partial melting of the rPET fibers during the processing (see Figure 2b,e).

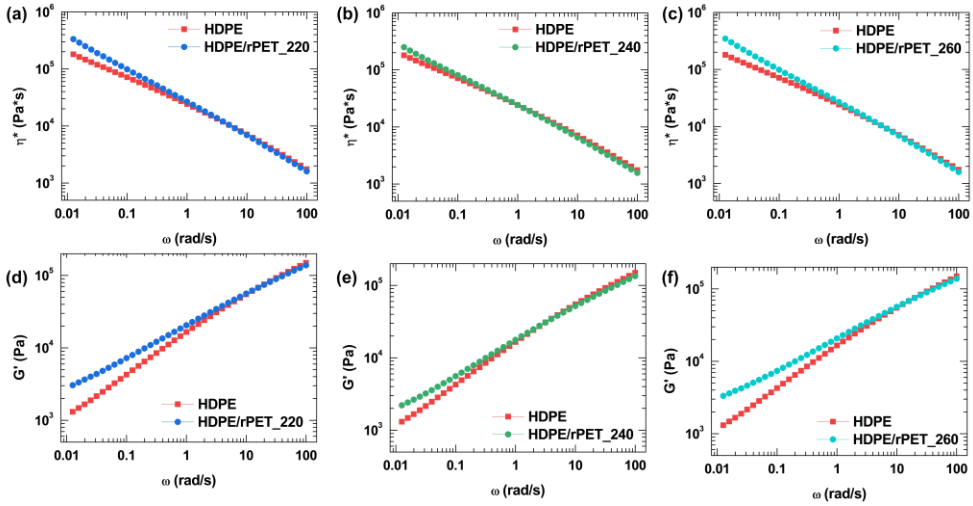

Figure 2. Trend of complex viscosity (η*) and of the storage modulus (G′) as a function of the frequency (ω) for HDPE/rPET processed at 220 (**a**,**d**), 240 (**b**,**e**) and 260 (**c**,**f**) °C. The rheological functions of the neat matrix are also reported.

Table 1. Fitting parameters of complex viscosity data using the Carreau–Yasuda rheological model.

	η_0 [Pa × s]	λ [s]	a	n
HDPE95/rPET5_220 °C	8.00×10^7	2.28×10^5	0.21	0.37
HDPE95/rPET5_240 °C	1.07×10^8	1.56×10^5	0.13	0.28
HDPE95/rPET5_260 °C	8.27×10^7	2.32×10^5	0.25	0.38

3.1.3. Mechanical Characterization

The main results of the tensile tests performed on the isotropic samples extruded at different temperatures are reported in Table 2. Regardless of the processing temperature, the presence of rPET induced an increase in the elastic modulus and a concurrent decrease in the elongation at break, while tensile strength underwent negligible changes. In particular, HDPE/rPET_260 showed the highest modulus with an increase of about 15% with respect to pristine HDPE, while the materials extruded at 220 and 240 °C exhibited a lower increment, accounting for 3% and 8%, respectively. On the other hand, while tensile strength was not significantly affected by the introduction of the dispersed phase, the elongation at break of all investigated rPET-containing systems was dramatically decreased as compared to the unfilled matrix. According to what is generally reported in the literature [18,23], the introduction of PET in a polymeric matrix usually implies higher values of elastic modulus and lower elongation at break, since the dispersed phase provides greater stiffness to the pristine matrix; at the same time, tensile strength undergoes negligible alterations or a minor diminishing with less than 50 wt% of PET. The differences noticed between the all-polymer systems processed at the three temperatures can be ascribed to their different morphology. In particular, for the processing carried out at 220 and 240 °C, the fibers were in the solid state or partially melted; therefore, the systems behaved like a typical composite, characterized by lower ductility and greater rigidity with respect to the neat matrix. At variance, the compounding temperature of 260 °C entailed the obtainment of a droplet-like morphology due to the modification of the rPET morphology from fibers to globular inclusion. This evolution of the material microstructure from a fiber-containing composite to a droplet-like blend involved an increase in the matrix/dispersed phase interfacial region, which in turn led to improved tensile properties.

Table 2. Mechanical properties of isotropic HDPE and HDPE/rPET all-polymer composites.

	E [MPa]	σ_{MAX} [MPa]	ε_{MAX} [%]
HDPE	541.8 ± 85.8	21.3 ± 1.6	500.5 ± 37.1
HDPE95/rPET5_220 °C	559.1 ± 69.9	22.0 ± 1.5	44.8 ± 9.1
HDPE95/rPET5_240 °C	588.4 ± 53.9	20.5 ± 0.6	43.8 ± 9.6
HDPE95/rPET5_260 °C	624.9 ± 60.3	20.3 ± 0.6	53.7 ± 5.7

3.2. Characterization of Stretched (Anisotropic) HDPE/rPET All-Polymer Materials

3.2.1. Hot-Stretched All-Polymer Composites

After the melt-compounding step, HDPE/rPET_260 °C was subjected to hot-stretching through the application of a uniaxial elongational flow on the molten extrudate at the exit of the extruder die. Figure 3a,b show the SEM micrographs of the obtained filaments characterized by low (i.e., 4) and high (i.e., 14) DR_H. Remarkable differences emerged when comparing the morphology of the filaments with that of the isotropic all-polymer composite obtained at the same processing temperature (see SEM micrograph shown in Figure 1d). Firstly, the main dimensions of the rPET inclusions in the hot-stretched filaments were remarkably lower than those in the isotropic sample. On the other hand, the distribution of the dimensions of the reinforcing phase particles tended to become more sharp, passing from extrudates to fibers. In particular, the main diameter of the rPET droplets in the isotropic extrudates ranged from 2.5 to 0.3 μm, whereas it changed to 1.3–0.25 μm and 0.7–0.15 μm for the filaments at low and high DR_H, respectively. Additionally, it is interesting to highlight that the rPET particle diameter further reduced when more intense hot-stretching was applied on the all-polymer composite filaments. The noticed differences can be ascribed to the effect of the applied elongational flow, which promoted the deformation and elongation of the dispersed phase particles and consequent break-up phenomena involving the rPET inclusions, ultimately causing a significant reduction in their average dimensions [24]. More importantly, in the all-polymer filaments that were hot-stretched at a high draw ratio, apart from the aforementioned reduction in the average dimensions of the rPET inclusions, a further phenomenon could be observed. In particular, as highlighted by the yellow circles in Figure 3b, the application of the elongational flow also promoted a droplet-to-fibril transition for the particles of the dispersed phase, which evolved from quasi-spherical domains in isotropic samples and low-DR_H filaments to anisotropic fibrils in high-DR_H materials. The observed alterations of the all-polymer composite morphology induced by the hot-stretching had a strong impact on the material tensile behavior, as observable in Figure 4, which shows the elastic modulus, maximum tensile strength and elongation at break for HDPE and HDPE/rPET_260 °C hot-stretched filaments at different DR_H. From a general point of view, upon the application of the elongational flow, both the pristine matrix and the all-polymer filaments exhibited enhanced tensile modulus and strength as a function of DR_H and a concurrent decrease in the elongation at break. These results can be ascribed to the progressive alignment of HDPE macromolecules and the evolution of the morphology of rPET resulting from the application of the elongational flow [17]. As expected, also considering the results of the tensile tests carried out on the isotropic specimens (see Table 2), the introduction of rPET caused a general increase in the tensile modulus and strength. More importantly, the differences in E and σ_{MAX} between the unfilled HDPE and the rPET containing systems tended to become more pronounced as the DR_H increased. This behavior can be explained considering the aforementioned decrease in the main size of the rPET inclusions and the droplet-to-fibril transition which the embedded domains underwent after being induced by hot-stretching. In other words, at low DR_H, the HDPE/rPET all-polymer system showed the typical morphology of an immiscible blend, notwithstanding the lower average sizes of the dispersed phase particles as compared to the correspondent isotropic sample. At variance, as the DR_H increased, two concurrent phenomena, both promoting enhanced stiffness and

strength, occurred: a continuous decrease in the main dimensions of rPET domains and their in situ fibrillation, leading to the formation of anisotropic structures. Furthermore, a progressive increase in the orientation degree of the fibrils along the stretching direction cannot be excluded. Surprisingly, the presence of rPET also caused an increase in the elongation at break with respect to pristine HDPE. Once again, the stretching-induced evolution of the material morphology can be invoked as responsible for this behavior. In fact, similarly to what reported in the literature for immiscible polymer blends [25,26], the formation of rPET microfibrils led to the establishment of a greater interfacial area between HDPE and the dispersed phase as compared to the isotropic materials, thereby allowing a more efficient matrix/dispersed phase stress transfer. In addition, due to the preferential orientation of the rPET fibrils along the same direction as the HDPE chains, the deformed rPET domains did not act as defects during the deformation of the material, enabling the obtainment of highly ductile filaments.

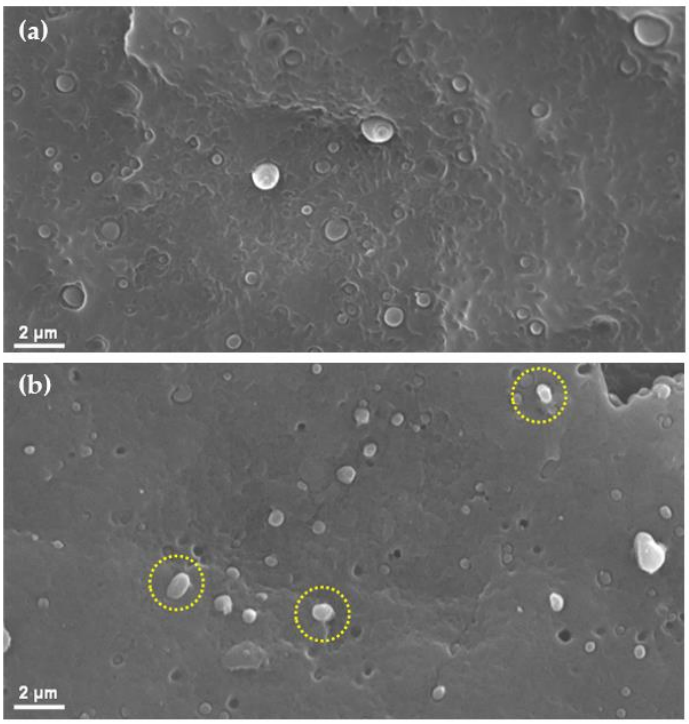

Figure 3. SEM micrographs for HDPE95/rPET5_260 °C hot-stretched filaments at DR_H 4 (**a**) and 14 (**b**).

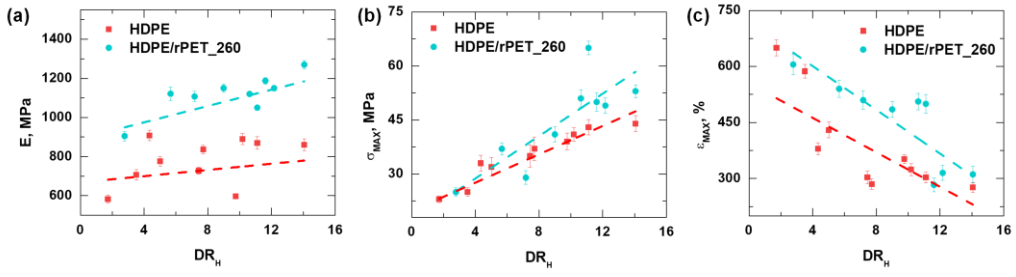

Figure 4. Tensile modulus (**a**), tensile strength (**b**) and elongation at break (**c**) for HDPE and HDPE/rPET filaments as a function of DR_H.

3.2.2. Cold-Stretched All-Polymer Composites

To explore the possible effect of the elongational flow applied in cold conditions on inducing further evolutions of the all-polymer system morphology, filaments of HDPE and HDPE95/rPET5_260 °C with a DR_H of 2 were further subjected to cold-stretching and the mechanical behavior of the so-obtained fibers was characterized through tensile tests. Figure 5a–c show the trend of elastic modulus, maximum tensile strength and elongation

at break for cold-stretched fibers at DR_C values ranging from 2 to 6. Similarly to what previously observed for the hot-stretched materials, as a result of the cold drawing, both HDPE and the all-polymer composite exhibited progressively increasing elastic modulus and tensile strength as a function of the cold draw ratio. At the same time, the material ductility decreased as the intensity of the applied stretching increased. Nevertheless, it is important to highlight that, especially for the all-polymer system, the enhancement of the modulus and tensile strength upon the application of the elongational flow at room temperature was significantly higher as compared to that achieved for the unfilled HDPE and, even more importantly, to that observed in the hot-stretched samples. As far as the unfilled HDPE is concerned, the trend of the tensile properties can be explained considering the further gradual orientation of the polymer macromolecules promoted by the application of cold-stretching. On the other hand, the tensile behavior of the all-polymer composite can be ascribed to the continuous evolution of the morphology of the rPET inclusions upon cold-stretching. In fact, similarly to what inferred for hot-stretched samples, also in this case, the dispersed phase particles (originally of spherical shape) tended to be deformed by the applied elongational flow, by transforming in ellipsoids and eventually into microfibrils, bringing about the observed variation in the mechanical properties. However, as also demonstrated in the literature [27,28], the application of the elongational flow in cold conditions was more effective than hot-stretching in inducing significant variation in the morphology of the dispersed phase inclusions. Therefore, a further amplification of the micro-fibrillation phenomenon already described in the case of hot-stretched samples can be inferred. Additionally, cold-stretching could also be effective in promoting a progressive orientation of the embedded anisotropic domains along the stretching direction. In fact, while the rPET domains were subjected to shape relaxation when the elongational flow was applied at high temperature, this phenomenon was suppressed in cold conditions, allowing for the achievement of a more oriented and anisotropic microstructure that, in turn, induced a more remarkable reinforcing effect.

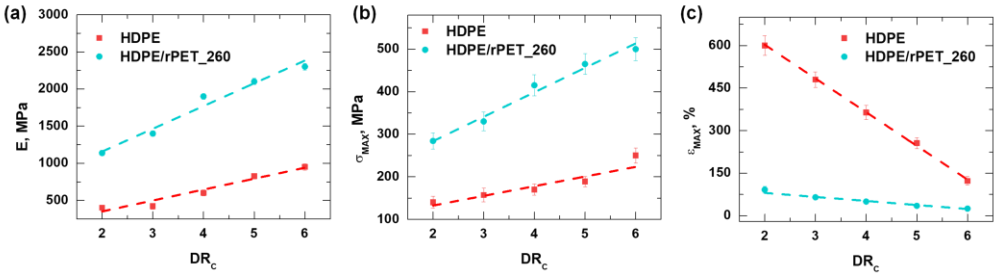

Figure 5. Tensile modulus (**a**), tensile strength (**b**) and elongation at break (**c**) for HDPE and HDPE/rPET filaments as a function of DR_C.

4. Conclusions

In this work, HDPE/rPET all-polymer composites were formulated through melt-compounding and subsequent hot- or cold-stretching, aiming at producing high-performance complex materials, entirely based on polymers, through a waste valorization strategy. In fact, rPET fibers recovered from discarded safety belts were exploited as reinforcing phase, aiming at providing a straightforward and industrially viable route for the upcycling of this waste material, the ultimate fate of which is usually incineration or landfill. In all, the obtained results demonstrated that the microstructure (hence, the final properties) of the designed all-polymer systems can be properly manipulated through the application of a uniaxial elongational flow, either in hot or cold conditions. Specifically, it was proven that upon hot-stretching, the main dimensions of the rPET domains embedded in the HDPE matrix tended to decrease; in addition, for the filaments with a high draw ratio, a sort of droplet-to-fibril transition was observed. The stretching-induced alteration of the material morphology promoted the enhancement of the tensile properties of the all-polymer system as compared to the unfilled matrix, testifying to the beneficial effect of the applied elonga-

tional flow on the mechanical behavior of the formulated HDPE/rPET system. Finally, it was also demonstrated that the tensile properties of the all-polymer system were even more enhanced when cold-stretching was applied, as a result of a further evolution of the material morphology towards the obtainment of a highly oriented anisotropic microstructure.

Author Contributions: Conceptualization, A.F. and R.A.; methodology, R.A.; validation, A.F. and R.A.; investigation, C.G.; data curation, C.G.; writing—original draft preparation, R.A. and C.G.; writing—review and editing, A.F; funding acquisition, R.A. All authors have read and agreed to the published version of the manuscript.

Funding: This research was funded by the MICS (Made in Italy—Circular and Sustainable) Extended Partnership and received funding from the European Union Next-GenerationEU (PIANO NAZIONALE DI RIPRESA E RESILIENZA (PNRR)—MISSIONE 4 COMPONENTE 2, INVESTIMENTO 1.3—D.D. 1551.11-10-2022, PE00000004). This manuscript reflects only the authors' views and opinions; neither the European Union nor the European Commission can be considered responsible for them.

Data Availability Statement: Data will be provided on request.

Conflicts of Interest: The authors declare no conflicts of interest.

References

1. Plastics Europe, Plastics–the Fast Facts 2023. Available online: https://plasticseurope.org/knowledge-hub/plastics-the-fast-facts-2023/ (accessed on 11 July 2024).
2. Bernagozzi, G.; Arrigo, R.; Ponzielli, G.; Frache, A. Towards effective recycling routes for polypropylene: Influence of a repair additive on flow characteristics and processability. *Polym. Degrad. Stab.* **2024**, *223*, 110714. [CrossRef]
3. Ignatyev, I.A.; Thielemans, W.; Vander Beke, B. Recycling of Polymers: A Review. *ChemSusChem* **2014**, *7*, 1579–1593. [CrossRef]
4. Vogt, B.D.; Stokes, K.K.; Kumar, S.K. Why is Recycling of Postconsumer Plastics so Challenging? *ACS Appl. Polym. Mater.* **2021**, *3*, 4325–4346. [CrossRef]
5. Ahmad, H.; Rodrigue, D. Upcycling of recycled polyethylene for rotomolding applications via dicumyl peroxide crosslinking. *J. Appl. Polym. Sci.* **2024**, *141*, e56236. [CrossRef]
6. European PET Bottle Platform. How to Keep a Sustainable PET Recycling Industry in Europe. 2024. Available online: https://www.epbp.org/ (accessed on 15 July 2024).
7. SYSTEMIQ. Achieving Circularity of PET Packaging and Polyester Textiles in Europe. 2023. Available online: https://www.systemiq.earth/pet-polyester/ (accessed on 15 July 2024).
8. Lei, Y.; Wu, Q.; Zhang, Q. Morphology and Properties of Microfibrillar Composites Based on Recycled Poly (Ethylene Terephthalate) and High Density Polyethylene. *Compos. Part A Appl. Sci. Manuf.* **2009**, *40*, 904–912. [CrossRef]
9. Singh, A.K.; Bedi, R.; Kaith, B.S. Composite materials based on recycled polyethylene terephthalate and their properties–A comprehensive review. *Compos. Part B Eng.* **2021**, *219*, 108928. [CrossRef]
10. Taepaiboon, P.; Junkasem, J.; Dangtungee, R.; Amornsakchai, T.; Supaphol, P. In Situ Microfibrillar-Reinforced Composites of Isotactic Polypropylene/Recycled Poly(Ethylene Terephthalate) System and Effect of Compatibilizer. *J. Appl. Polym. Sci.* **2006**, *102*, 1173–1181. [CrossRef]
11. Kuzmanović, M.; Delva, L.; Cardon, L.; Ragaert, K. Relationship between the Processing, Structure, and Properties of Microfibrillar Composites. *Adv. Mater.* **2020**, *32*, 2003938. [CrossRef]
12. Fakirov, S. Nano-/microfibrillar polymer–polymer and single polymer composites: The converting instead of adding concept. *Compos. Sci. Technol.* **2013**, *89*, 211–225. [CrossRef]
13. Fakirov, S.; Bhattacharyya, D.; Shields, R.J. Nanofibril reinforced composites from polymer blends. *Colloid Surf. A* **2008**, *313–314*, 2–8. [CrossRef]
14. Arrigo, R.; Malucelli, G.; La Mantia, F.P. Effect of the Elongational Flow on the Morphology and Properties of Polymer Systems: A Brief Review. *Polymers* **2021**, *13*, 3529. [CrossRef] [PubMed]
15. Sombatdee, S.; Amornsakchai, T.; Saikrasun, S. Reinforcing performance of recycled PET microfibrils in comparison with liquid crystalline polymer for polypropylene based composite fibers. *J. Polym. Res.* **2012**, *19*, 9843. [CrossRef]
16. Liu, Q.; Zhang, X.; Jia, D.; Yin, J.; Lei, J.; Xu, L.; Lin, H.; Zhong, G.; Li, Z. In situ nanofibrillation of polypropylene/polyethylene/poly(ethylene terephthalate) ternary system: A strategy of upgrade recycling. *Polymer* **2023**, *269*, 125729. [CrossRef]
17. Gnoffo, C.; Arrigo, R.; Sisani, M.; Frache, A. Elongational flow-induced microstructure evolutions in polypropylene/layered double hydroxides nanocomposites. *Polym. Compos.* **2024**, *45*, 6606–6617. [CrossRef]
18. Evstatiev, M.; Fakirov, S.; Krasteva, B.; Friedrich, K.; Covas, J.A.; Cunha, A.M. Recycling of Poly(Ethylene Terephthalate) as Polymer-Polymer Composites. *Polym. Eng. Sci.* **2002**, *42*, 826–835. [CrossRef]

19. Li, Z.; Yang, M.; Feng, J.; Yang, W.; Huang, R. Morphology of in Situ Poly(Ethylene Terephthalate)/Polyethylene Microfiber Reinforced Composite Formed via Slit-Die Extrusion and Hot-Stretching. *Mater. Res. Bull.* **2002**, *37*, 2185–2197. [CrossRef]
20. Vittorias, I.; Lilge, D.; Baroso, V.; Wilhelm, M. Linear and Non-Linear Rheology of Linear Polydisperse Polyethylene. *Rheol. Acta* **2011**, *50*, 691–700. [CrossRef]
21. Rizvi, A.; Park, C.B.; Favis, B.D. Tuning Viscoelastic and Crystallization Properties of Polypropylene Containing In-Situ Generated High Aspect Ratio Polyethylene Terephthalate Fibrils. *Polymer* **2015**, *68*, 83–91. [CrossRef]
22. Casamento, F.; D'Anna, A.; Arrigo, R.; Frache, A. Rheological Behavior and Morphology of Poly(Lactic Acid)/Low-Density Polyethylene Blends Based on Virgin and Recycled Polymers: Compatibilization with Natural Surfactants. *J. Appl. Polym. Sci.* **2021**, *138*, 50590. [CrossRef]
23. Akshaya, E.M.; Palaniappan, R.; Sowmya, C.F.; Rasana, N.; Jayanarayanan, K. Properties of Blends from Polypropylene and Recycled Polyethylene Terephthalate Using a Compatibilizer. *Mater. Today Proc.* **2020**, *24*, 359–368. [CrossRef]
24. Shields, R.J.; Bhattacharyya, D.; Fakirov, S. Oxygen Permeability Analysis of Microfibril Reinforced Composites from PE/PET Blends. *Comp. Part A Appl. Sci. Manuf.* **2008**, *39*, 940–949. [CrossRef]
25. La Mantia, F.P.; Fontana, P.; Morreale, M.; Mistretta, M.C. Orientation induced brittle-ductile transition in a polyethylene/polyamide 6 blend. *Polym. Test.* **2014**, *36*, 20–23. [CrossRef]
26. Perin, D.; Rigotti, D.; Fredi, G.; Papageorgiou, G.Z.; Bikiaris, D.N.; Dorigato, A. Innovative Bio-based Poly(Lactic Acid)/Poly(Alkylene Furanoate)s Fiber Blends for Sustainable Textile Applications. *J. Polym. Environ.* **2021**, *29*, 3948–3963. [CrossRef]
27. Fakirov, S.; Bhattacharyya, D.; Lin, R.; Fuchs, C.; Friedrich, K. Contribution of Coalescence to Microfibril Formation in Polymer Blends during Cold Drawing. *J. Macromol. Sci. B* **2007**, *46*, 183–194. [CrossRef]
28. Mi, D.; Wang, Y.; Kuzmanovic, M.; Delva, L.; Jiang, Y.; Cardon, L.; Zhang, J.; Ragaert, K. Effects of Phase Morphology on Mechanical Properties: Oriented/Unoriented PP Crystal Combination with Spherical/Microfibrillar PET Phase. *Polymers* **2019**, *11*, 248. [CrossRef] [PubMed]